THE ASTROPHYSICAL JOURNAL, SUPPLEMENT SERIES, 105:401–405, 1996 August

ULTRAVIOLET AND INFRARED REFRACTIVE INDICES OF AMORPHOUS SILICATES

A. SCOTT AND W. W. DULEY[1]
Guelph-Waterloo Program for Graduate Work in Physics, University of Waterloo, Waterloo, ON, Canada N2L 3G1
Received 1995 October 20; accepted 1996 February 1

ABSTRACT

Thin films of amorphous magnesium silicates with compositions similar to those of enstatite ($MgSiO_3$) and forsterite (Mg_2SiO_4) have been deposited using excimer laser ablation of the parent materials. Refractive indices n and k for these materials have been derived from optical transmission and reflection spectra together with Kramers-Kronig analysis. Measured refractive indices are reported for the range 0.12–17.5 μm and are extended to shorter and longer wavelengths by fitting to data reported from other experiments and to theoretical predictions. The overall n, k data set is consistent with Kramers-Kronig. We find that the strength of the 10 μm band in these amorphous materials is comparable to that customarily assumed for astronomical silicates. In addition, the strength of absorption in the vacuum ultraviolet is similar to previous estimates. We find that the onset of strong UV absorption in our samples occurs near that of "astronomical silicate" and is only slightly dependent on composition. The emissivity of small particles of amorphous forsterite, calculated using our measured n, k, is found to peak at 9.6 μm.

Subject headings: dust, extinction — infrared: general — molecular data — ultraviolet: general

1. INTRODUCTION

For some time, silicates have been proposed as a major component of interstellar dust (see the review by Whittet 1992). Due to conditions in the interstellar medium, this dust is likely to be formed in an amorphous state. Evidence for the presence of silicates in interstellar clouds derives primarily from the observation of infrared spectral features at 9.7 and 18 μm (Penman 1976; Forrest, McCarthy, & Houck 1979; Willner et al. 1982; Olnon & Raimond 1986; Whittet et al. 1988). Such silicates are expected to contain iron and magnesium, since these are the only elements which have sufficient abundance to combine efficiently with silicon. A lack of sharp structure in spectra of the 9.7 μm band suggests that silicate grains have an amorphous, disordered structure (Day 1979, 1981; Dorschner & Henning 1986), while the observation of linear polarization in these IR bands indicates that silicate grains are elongated and aligned (Aitken, Smith, & Roche 1989).

Silicate grains with a range of sizes are an important component of all grain models and are postulated to contribute significantly to extinction at all wavelengths due to a combination of absorption and scattering (Greenberg 1989; Mathis 1989; Williams 1989). Large (0.1–0.2 μm) silicate grains are suggested as the source of polarization at wavelengths in the visible and near-UV, while a population of much smaller (0.01 μm) grains is required to produce the rapid rise in far UV extinction seen in many interstellar spectra. A recent discussion of the effect of small silicate particles on polarization in the far-UV (Kim & Martin 1995) has concluded that an excess of very small aligned silicate particles may be required to fit polarization observations in the region $\lambda^{-1} > 6$ μm^{-1} unless the optical constants of the silicate material are quite different from that customarily used for "astronomical silicate" (Draine & Lee 1984) which are based on a crystalline olivine. There have been a number of laboratory measurements of refractive indices for silicates with compositions similar to those expected for interstellar dust (Huffman 1970; Huffman & Stapp 1971; Krätschmer & Huffman 1979; Jager et al. 1994; Dorschner et al. 1995), but no experimental data have been reported for amorphous silicates over a spectral range which includes both the 9.7 μm infrared band and fundamental edge absorption at wavelengths shorter than 170 nm.

In this paper we report on the measurement of refractive indices for amorphous silicates with compositions like those of enstatite and forsterite over a wavelength range which includes both IR vibrational and far-UV electronic absorption bands. We compare the results of these measurements to indices for astronomical silicate and find that our measured indices are similar, but not identical, to that based on crystalline olivine.

2. EXPERIMENTAL

Samples for infrared measurements were prepared by 308 nm excimer laser ablation of geological samples of polycrystalline forsterite (Mg_2SiO_4) and enstatite (Mg_2SiO_3). Ablation products were deposited on a KCl window held at room temperature in a vacuum of 10^{-5} torr. Excimer laser deposition of refractory solids under these conditions with UV radiation is known to yield thin films with a composition close to that of the parent material (Duley 1996). Material removal occurs in an ablative interaction whereby the parent material is dissociated and emerges from the irradiated surface in a plume which is primarily atomic and molecular, with cluster and cluster ions (Geohagen 1993; Butt & Wantuck 1993; Webb et al. 1993) but without the presence of macroscopic particles. The resulting deposit generally has a composition which is close to that of the parent material.

Laser radiation was obtained from a pulsed XeCl excimer laser and was focused to a 1 mm diameter spot on the crystalline mineral. The pulse energy was 100 mJ in a pulse of 30 ns duration. Samples were deposited over a period of

[1] wwduley@physics.watstar.uwaterloo.ca.

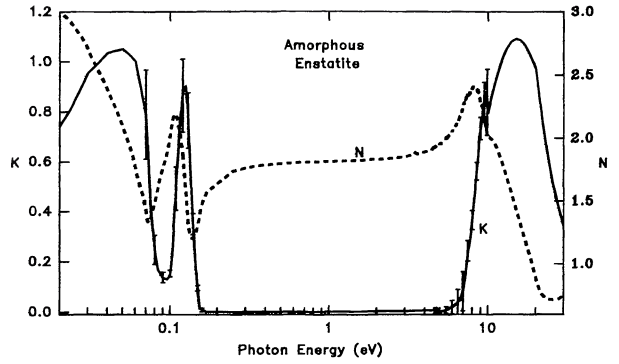

FIG. 1.—Refractive indices n, k derived from optical measurements on amorphous films of enstatite ($MgSiO_3$).

120 minutes with the laser operating at 10 Hz and were typically 1–2 μm thick. These samples were then transferred to a Bomem model MB100 FTIR spectrometer, at which transmission spectra were measured in the region from 550 to 4000 cm^{-1} and ratioed to transmission spectra of the KCl blank.

Amorphous enstatite and forsterite films for UV measurements were obtained by ablating crystalline samples onto 1 mm thick magnesium flouride windows using the same process as above but with much shorter deposition times ($\sim$3 minutes). Transmission spectra of the resulting films were measured in situ. UV radiation was obtained from a Helma Cells model V05 ruggedized deuterium lamp with a magnesium fluoride window mounted on the entrance slit to a 0.2 m Minuteman Labs Inc. model 302-VM scanning monochromator evacuated to approximately 10^{-5} torr by a liquid nitrogen trapped oil diffusion pump. The wavelength range was 122–300 nm with a resolution of 2.4 nm. A thin magnesium fluoride window separated the monochromator chamber from the sample chamber. A beam splitter was used to reflect part of the incident beam into a reference channel monitored by an EMI 9558QB photomultiplier tube with a sodium salicylate coated entrance window. A magnesium fluoride lens focused the light onto the sample, and the intensity of radiation passing through the sample was measured using a Hamamatsu R189 photomultiplier tube with a similar sodium salicylate coated window. Signals from both channels were recorded with a photon-counting system operating in ratio mode. The resulting data were logged by a microprocessor which controlled the wavelength of the monochromator by means of a motor/encoder system.

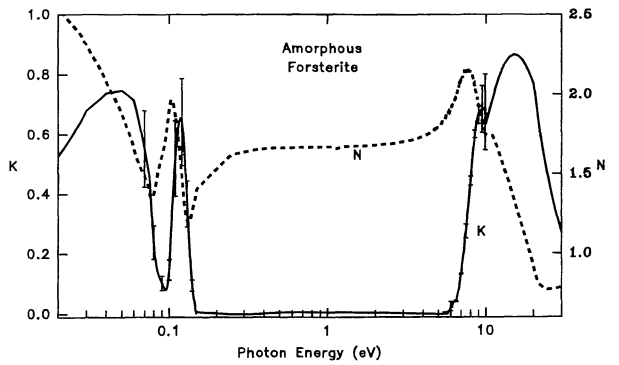

FIG. 2.—Refractive indices n, k derived from optical measurements on amorphous films of forsterite (Mg_2SiO_4).

Before the samples were deposited, a blank spectrum was collected under standard conditions. During deposition, the phototubes were turned off to prevent damage from scattered laser radiation. After deposition of a sample and rewarming of the electronics, the transmission of the sample was measured under identical conditions as that of the blank spectrum.

Electron-excited X-ray emission was used to compare the elemental composition of deposited films with those of the parent material. These experiments indicated that elemental ratios in the parent material were preserved in films prepared by laser ablation. The sample thicknesses of the UV films were found through thin-film ellipsometry and were typically 18.5–34 nm. These thicknesses were confirmed using cross-sectional scanning electron microscopy. Films used for IR spectra were 1.5–2 μm thick as measured by cross-sectional electron microscopy. Increased surface roughness in thicker films made it difficult to use ellipsometric techniques.

3. RESULTS

Figures 1 and 2 show the refractive indices n and k derived from transmission measurements in the IR and the UV for amorphous enstatite and forsterite films, respectively. Error bars are shown to reflect the standard deviation of thickness measurements or the range of k observed in the films. The experimental data cover the range from 0.07 to 0.43 eV (0.057–0.347 μm^{-1}) in the infrared and from 4.7 to 10 eV (3.80–8.08 μm^{-1}) in the UV. To calculate refractive indices, preliminary values of k were first found using the assumption that reflection and interference effects were negligible. Kramers-Kronig analysis was then used to find n in the same region. These values were used in an iterative numerical procedure, along with the known thickness to modify k using the exact formula for the transmission of a thin film (Heavens 1965). Finally, n values were updated using Kramers-Kronig analysis to obtain a consistent set of n and k. Calculated k-values from several films with accurately measured thicknesses were averaged and were used to calculate n via Kramers-Kronig. Values for k outside the spectral range of our measurements were estimated using data for astronomical silicate (Draine & Lee 1984) (0–0.07 eV, >20 eV) and from reflection measurements on crystalline forsterite (Nitsan & Shankland 1976) (10–20 eV) normalized to our experimental values of k at 0.07 and 10 eV. The full data set is given in numerical form in Table 1.

4. DISCUSSION

Values for k measured for a forsterite film are compared to those for astronomical silicate from Draine & Lee (1984) in Figure 3. In the ultraviolet, the onset of absorption is caused by electronic transitions across the band gap to energy levels near the edge of the conduction band. An absorption tail extending from the band gap to lower energies is typically present in amorphous materials and reflects the variation in bond energy that may occur in such

TABLE 1

OPTICAL CONSTANTS n AND k OF AMORPHOUS FILMS DEPOSITED BY LASER ABLATION OF MAGNESIUM SILICATES IN VACUUM

$1/\lambda$ (μm^{-1})	E (eV)	AMORPHOUS FORSTERITE k	AMORPHOUS FORSTERITE n	AMORPHOUS ENSTATITE k	AMORPHOUS ENSTATITE n
0.0162.....	0.02	0.529	2.54	0.743	3.03
0.0242.....	0.03	0.681	2.31	0.956	2.7
0.0323.....	0.04	0.738	2.09	1.04	2.38
0.0404.....	0.05	0.747	1.88	1.05	2.09
0.0485.....	0.06	0.715	1.66	1	1.77
0.0566.....	0.07	0.552	1.49	0.79	1.43
0.0646.....	0.08	0.239	1.37	0.249	1.49
0.0727.....	0.09	0.104	1.61	0.137	1.76
0.0808.....	0.1	0.147	1.9	0.153	2.01
0.0889.....	0.11	0.545	1.84	0.535	2.17
0.0945.....	0.117	0.655	1.59	0.799	1.99
0.097	0.12	0.642	1.47	0.865	1.86
0.101	0.125	0.538	1.29	0.912	1.59
0.105	0.13	0.368	1.2	0.766	1.33
0.113	0.14	0.0956	1.27	0.352	1.21
0.121	0.15	0.00683	1.41	0.0951	1.31
0.129	0.16	0.00615	1.43	0.00808	1.48
0.137	0.17	0.00547	1.45	0.000112	1.56
0.145	0.18	0.00478	1.47	9.79E−005	1.58
0.154	0.19	0.0041	1.49	8.39E−005	1.61
0.162	0.2	0.00342	1.51	6.99E−005	1.63
0.17	0.21	0.00273	1.54	5.6E−005	1.65
0.178	0.22	0.00205	1.56	4.2E−005	1.67
0.186	0.23	0.00137	1.58	2.8E−005	1.69
0.194	0.24	0.000683	1.6	1.4E−005	1.71
0.202	0.25	0	1.62	0	1.74
0.21	0.26	0	1.62	0	1.74
0.218	0.27	0	1.63	0	1.74
0.226	0.28	0	1.63	0	1.75
0.234	0.29	0	1.63	0	1.75
0.242	0.3	0	1.64	0	1.76
0.251	0.31	0	1.64	0	1.76
0.259	0.32	0	1.64	0	1.76
0.267	0.33	0	1.64	0	1.77
0.275	0.34	0	1.65	0	1.77
0.283	0.35	0	1.65	0	1.78
0.291	0.36	0.000432	1.65	0	1.78
0.299	0.37	0.000864	1.65	0	1.78
0.307	0.38	0.0013	1.65	0	1.78
0.315	0.39	0.00173	1.65	0	1.78
0.323	0.4	0.00216	1.66	0	1.78
0.646	0.8	0.0062	1.67	0.000542	1.81
0.97	1.2	0.00557	1.66	0.00122	1.82
1.29	1.6	0.00493	1.67	0.0019	1.82
1.62	2	0.00429	1.68	0.00258	1.83
1.94	2.4	0.00366	1.68	0.00325	1.84
2.26	2.8	0.00302	1.69	0.00393	1.85
2.59	3.2	0.00239	1.7	0.00461	1.86
2.91	3.6	0.00175	1.72	0.00529	1.87
3.23	4	0.00111	1.73	0.00597	1.89
3.31	4.1	0.000954	1.74	0.00613	1.89
3.39	4.2	0.000795	1.74	0.0063	1.9
3.47	4.3	0.000636	1.75	0.00647	1.9
3.57	4.4	0.000477	1.75	0.00664	1.91
3.64	4.5	0.000318	1.76	0.00681	1.92
3.72	4.6	0.000159	1.76	0.00698	1.93
3.8.....	4.7	0	1.77	0.00715	1.93
3.88	4.8	0	1.78	0.0129	1.94
3.96	4.9	0	1.79	0.0113	1.95
4.04	5	0	1.8	0.00166	1.95
4.12	5.1	0	1.8	0.00272	1.96
4.2.....	5.2	0	1.81	0.00384	1.97
4.28	5.3	0	1.82	0.00521	1.98
4.36	5.4	5.54E−007	1.83	0.00595	1.99
4.44	5.5	0.0035	1.84	0.00883	2
4.53	5.6	0.00157	1.86	0.00956	2.01
4.61	5.7	2.5E−006	1.87	0.0111	2.02
4.69	5.8	0.0108	1.88	0.0163	2.03

TABLE 1—*Continued*

$1/\lambda$ (μm^{-1})	E (eV)	AMORPHOUS FORSTERITE k	AMORPHOUS FORSTERITE n	AMORPHOUS ENSTATITE k	AMORPHOUS ENSTATITE n
4.77.....	5.9	0.00874	1.89	0.0176	2.05
4.85.....	6	0.0266	1.91	0.0194	2.06
4.93.....	6.1	0.0258	1.93	0.0216	2.07
5.01.....	6.2	0.039	1.94	0.0257	2.09
5.09.....	6.3	0.0417	1.95	0.0301	2.1
5.17.....	6.4	0.0417	1.96	0.0323	2.12
5.25.....	6.5	0.0431	1.98	0.037	2.14
5.33.....	6.6	0.0567	2.01	0.0462	2.16
5.41.....	6.7	0.0762	2.03	0.0449	2.18
5.49.....	6.8	0.0839	2.05	0.0601	2.2
5.58.....	6.9	0.122	2.07	0.0726	2.22
5.66.....	7	0.134	2.09	0.0821	2.25
5.74.....	7.1	0.177	2.1	0.112	2.27
5.82.....	7.2	0.19	2.11	0.13	2.3
5.9	7.3	0.208	2.13	0.162	2.32
5.98.....	7.4	0.264	2.14	0.191	2.34
6.06.....	7.5	0.276	2.14	0.244	2.35
6.14.....	7.6	0.317	2.14	0.255	2.36
6.22.....	7.7	0.342	2.16	0.278	2.35
6.3	7.8	0.374	2.14	0.3	2.37
6.38.....	7.9	0.409	2.14	0.33	2.39
6.46.....	8	0.445	2.14	0.367	2.4
6.55.....	8.1	0.481	2.13	0.415	2.4
6.63.....	8.2	0.513	2.11	0.45	2.4
6.71.....	8.3	0.549	2.09	0.485	2.4
6.79.....	8.4	0.569	2.07	0.525	2.4
6.87.....	8.5	0.601	2.05	0.564	2.39
6.95.....	8.6	0.62	2.02	0.601	2.38
7.03.....	8.7	0.634	2	0.641	2.37
7.11.....	8.8	0.648	1.97	0.68	2.34
7.19.....	8.9	0.659	1.95	0.715	2.32
7.27.....	9	0.666	1.92	0.735	2.29
7.35.....	9.1	0.672	1.9	0.76	2.27
7.43.....	9.2	0.676	1.88	0.782	2.25
7.52.....	9.3	0.679	1.87	0.814	2.22
7.6	9.4	0.681	1.85	0.834	2.19
7.68.....	9.5	0.684	1.83	0.84	2.15
7.76.....	9.6	0.685	1.81	0.851	2.13
7.84.....	9.7	0.685	1.8	0.858	2.1
7.92.....	9.8	0.688	1.78	0.868	2.05
8	9.9	0.675	1.75	0.84	2.16
8.08.....	10	0.634	1.75	0.794	2.02
8.89.....	11	0.72	1.74	0.909	1.97
9.7	12	0.787	1.65	0.993	1.84
10.5.....	13	0.831	1.55	1.05	1.71
11.3.....	14	0.857	1.44	1.08	1.57
12.1.....	15	0.866	1.34	1.09	1.44
12.9.....	16	0.863	1.25	1.09	1.32
13.7.....	17	0.848	1.16	1.07	1.21
14.5.....	18	0.826	1.08	1.04	1.11
15.4.....	19	0.8	0.998	1.01	1
16.2.....	20	0.771	0.906	0.972	0.887
17.....	21	0.681	0.834	0.859	0.795
17.8.....	22	0.605	0.801	0.763	0.754
18.6.....	23	0.54	0.784	0.681	0.731
19.4.....	24	0.485	0.775	0.611	0.72
20.2.....	25	0.437	0.772	0.551	0.715
21.....	26	0.395	0.775	0.499	0.715
21.8.....	27	0.359	0.775	0.453	0.718
22.6.....	28	0.327	0.779	0.413	0.723
23.4.....	29	0.299	0.784	0.378	0.735

materials (Madan & Shaw 1988). This tail is observed to a limited extent as an increase in k at photon energies less than 8 eV in our spectra of both forsterite and enstatite but is not as noticeable as in astronomical silicate. Impurities,

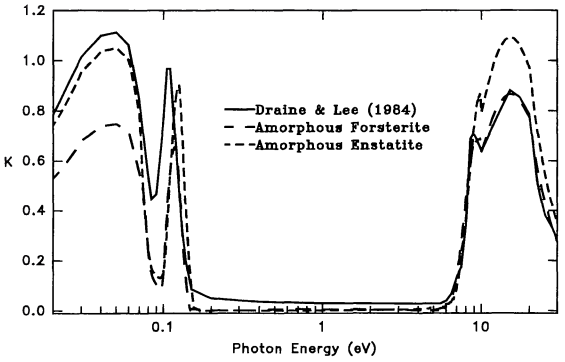

FIG. 3.—Comparison of k derived from experimental data with that of Draine & Lee (1984) for astronomical silicate.

such as the transition metal ions Fe^{2+}, Fe^{3+}, Mn^{2+}, Ni^{2+}, etc., may also absorb in this region (Nitsan & Shankland 1976). The presence of Fe, in particular, will shift the onset of UV absorption to lower photon energies. Dorschner et al. (1995) have shown that increasing Fe content in pyroxene and olivine glasses also tends to increase the relative absorption in the trough between the 10 and 20 μm IR peaks, while increasing absorption in the near IR and shorter wavelengths.

In the infrared, the 10 μm SiO absorption peak in enstatite and forsterite films has approximately the same width as derived by Draine & Lee (1984), but the peak value of k occurs at shorter wavelength. Mie scattering calculations using our measured values of n and k give peak absorptivities at 9.59 and 10.06 μm for enstatite and forsterite particles (Figs. 4 and 5, respectively) in the small particle limit, where peak wavelengths are relatively insensitive to particle size and shape. Both resonances move to longer wavelength with an increase in particle size.

Absorption coefficients for small spherical particles of both types of silicates are compared in Figure 6 to those for silicate particles in the two distinct interstellar environments described by Pégourie & Papoular (1985). The normalized absorption coefficient of dust in the optically thin circumstellar envelope of the Mira star U Tel as determined from *IRAS* low-resolution spectrometer (LRS) spectra (Dorschner et al. 1995) is reasonably well simulated by small particles of amorphous forsterite. This is in agreement with thermodynamic calculations which suggest that solid Mg_2SiO_4 (forsterite) forms before $MgSiO_3$ (enstatite) in a

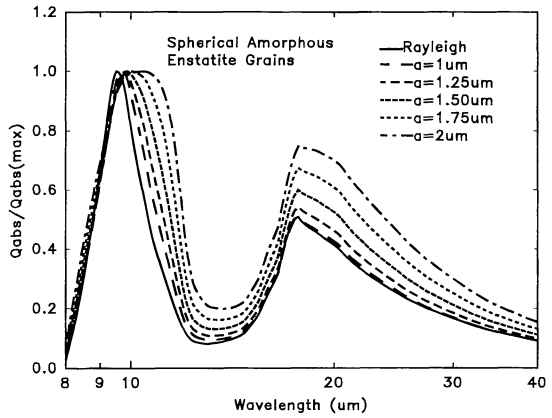

FIG. 4.—Wavelength dependence of Q_{abs} for amorphous enstatite particles.

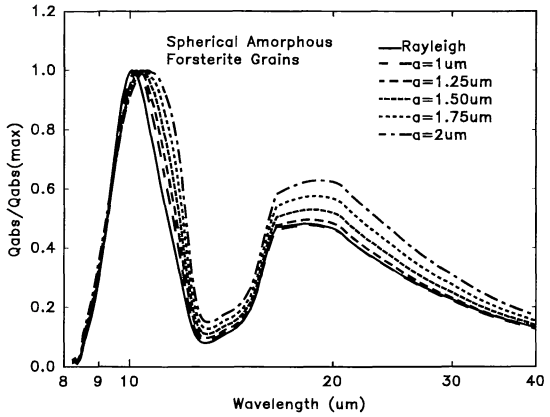

FIG. 5.—Wavelength dependence of Q_{abs} for amorphous forsterite particles.

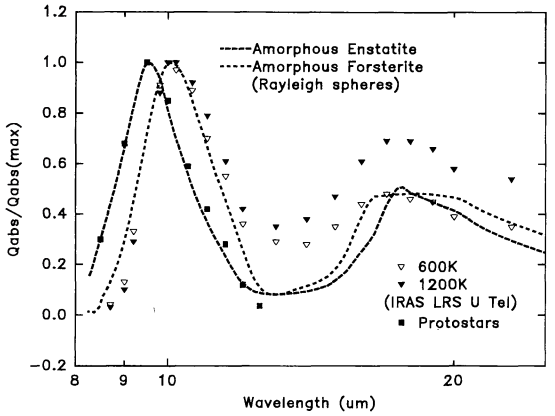

FIG. 6.—Comparison of normalized absorption coefficients for amorphous enstatite and forsterite particles with that of silicate dust in U Tel (Dorschner et al. 1995) and protostars (Pégourié & Papoular 1985).

cooling atmosphere (Grossman 1972; Larimer 1979). Eventually, reaction with the gas will transform the olivine to pyroxene. Figure 6 also shows a good fit between the absorption coefficient of enstatite and the opacity of silicate dust in protostars (Pégourié & Papoular 1985). On average, the dust surrounding protostellar objects could be older than dust observed in Mira stars and would be expected to contain a higher proportion of pyroxenes such as enstatite.

The absorbance at 10 μm in our silicate samples is somewhat less intense than that derived by Draine & Lee (1984). However, the absolute strength of the SiO stretch band in silicates is somewhat uncertain, since it depends not only on composition but on crystal structure and on temperature (Day 1976). The amorphous nature of our enstatite and forsterite films is confirmed by the observed width and lack of structure within the 10 μm peak as well as by scanning electron microscope studies. These results suggest that films prepared by laser ablation can reproduce some of the properties of interstellar grains as inferred from observational data. This experimental technique lends itself to the preparation of films of mixed composition, and we are examining the effect of including iron and other metals in our amorphous forsterite and enstatite solids.

This research was supported by grants from the NSERC of Canada.

REFERENCES

Aitken, D. K., Smith, C. H., & Roche, P. F. 1989, MNRAS, 236, 919
Butt, D. P., & Wartuck, P. J. 1993, Mat. Res. Soc. Symp. Proc., 285, 81
Day, K. L. 1976, ApJ, 210, 614
———. 1979, ApJ, 234, 158
———. 1981, ApJ, 426, 110
Dorschner, J. Begemann, B., Henning, Th., Jäger, C., & Mutschke, H. 1995, A&A, 300, 503
Dorschner, J., & Henning, Th. 1986, Ap&SS, 128, 47
Draine, B., & Lee, H. M., 1984, ApJ, 285, 89
Duley, W. W. 1996, in UV Lasers: Effects and Applications in Materials Science (Cambridge: Cambridge Univ. Press), in press
Forrest, W. J., McCarthy, J. F., & Houck, J. R. 1979, ApJ, 233, 611
Geohagen, D. B., 1993, Mat. Res. Soc. Symp. Proc. 285, 27
Greenberg, J. M. 1989, in IAU Symp. 135, Interstellar Dust, ed. L. J. Allamandola & A. G. G. M. Tielens (Dordrecht: Kluwer), 345
Grossman, L. 1972, Geochim, & Cosmochim. Acta, 36, 597
Heavens, O. S. 1965, Optical Properties of Thin Solid Films (New York: Dover)
Huffman, D. R. 1970, ApJ, 161, 1157
Huffman, D. R., & Stapp, J. L. 1971, Nature Phys. Sci., 229, 45
Jager, C., Mutschke, H., Begemann, B., Dorschner, J., & Henning, Th. 1994, A&A, 292, 641
Kim, S., & Martin, P. G. 1995, ApJ, 442, 172
Krätschmer, W., & Huffman, D. R. 1979, Ap&SS, 61, 195
Larimer, J. W. 1979, Ap&SS, 65, 351
Madan, A., & Shaw, M. P. 1988, The Physics and Applications of Amorphous Semiconductors (New York: Academic Press)
Mathis, J. 1989, in IAU Symp. 135, Interstellar Dust, ed. L. J. Allamandola & A. G. G. M. Tielens (Dordrecht: Kluwer 357)
Nitsan, U., & Shankland, T. J., 1976, Geophys. J., 45, 59
Olnon, F. M., & Raimond, E., ed. 1986, A&AS, 65, 607
Pégourié, B., & Papoular, R. 1985, A&A, 142, 451
Penman, J. M. 1976, MNRAS, 175, 149
Webb, R. L., Jensen, L. C., Langford, S. C., & Dickenson, J. T., 1993, J. Appl. Phys., 74, 2338
Whittet, D. C. B. 1992, Dust in the Galactic Environment (Bristol: IOP Publishing)
Whittet, D. C. B. et al. 1988, MNRAS, 233, 321
Williams, D. A. 1989, in IAU Symp. 135, Interstellar Dust, ed. L. J. Allamandola & A. G. G. M. Tielens (Dordrecht: Kluwer), 367
Willner, S. P., et al. 1982, ApJ, 253, 174